Scientific Research Publishing

American Journal of Analytical Chemistry, 2023, 14, 149-174
https://www.scirp.org/journal/ajac
ISSN Online: 2156-8278
ISSN Print: 2156-8251

Microwave-Assisted Au and Ag Nanoparticle Synthesis: An Energy Phase-Space Projection Analysis

Victor J. Law*, Denis P. Dowling

School of Mechanical and Materials Engineering, University College Dublin, Dublin, Ireland
Email: *viclaw66@gmail.com

How to cite this paper: Law, V.J. and Dowling, D.P. (2023) Microwave-Assisted Au and Ag Nanoparticle Synthesis: An Energy Phase-Space Projection Analysis. *American Journal of Analytical Chemistry*, **14**, 149-174.
https://doi.org/10.4236/ajac.2023.144009

Received: March 23, 2023
Accepted: April 24, 2023
Published: April 27, 2023

Abstract

Microwave-assisted synthesis of gold and silver nanoparticles, as a function of Green Chemistry, non Green Chemistry, and four applicator types are reported. The applicator types are Domestic microwave ovens, commercial temperature controlled microwave chemistry ovens (TCMC), digesters, and axial field helical antennae. For each of these microwave applicators the process energy budget where estimated (Watts multiplied by process time = kJ) and energy density (applied energy divided by suspension volume = $kJ \cdot ml^{-1}$) range between 180 ± 176.8 kJ, and 79.5 ± 79 $kJ \cdot ml^{-1}$, respectively. The axial field helical field antenna applicator is found to be the most energy efficient (0.253 $kJ \cdot m^{-1}$ per kJ, at 36 W). Followed by microwave ovens (4.47 ± 3.9 $kJ \cdot ml^{-1}$ per 76.83 ± 39 kJ), and TCMC ovens (2.86 ± 2.3 $kJ \cdot m^{-1}$ per 343 ± 321.5 kJ). The digester applicators have the least energy efficiency (36.2 ± 50.7 $kJ \cdot m^{-1}$ per 1010 ± 620 kJ). A comparison with reconstructed 'non-thermal' microwave oven inactivation microorganism experiments yields a power-law signature of n = 0.846 (R^2 = 0.7923) four orders of magnitude. The paper provides a discussion on the Au and Ag nanoparticle chemistry and bio-chemistry synthesis aspects of the microwave applicator energy datasets and variation within each dataset. The visual and analytical approach within the energy phase-space projection enables a nanoparticle synthesis route to be systematically characterized, and where changes to the synthesis are to be mapped and compared directly with historical datasets. In order to help identify lower cost nanoparticle synthesis, in addition to potentially reduce synthesis energy to routes informed changes to potentially reduce synthesis energy budget, along with nanoparticle morphology and yield.

Keywords

Turkevich, Microwave-Assisted Synthesis, Ag, Au, Hydroxyapatite,

Nanoparticle, Functionalization, Energy Phase-Space Projection

1. Introduction

Gold (Au), silver (Ag) particles with a grain size < 100 nm in at least one dimension are collectively part of the noble metal nanoparticle family that exhibit unique properties when compared to bulk materials. Today (2023) noble metal and ceramic nanoparticles are designed with specific optical, electrical, magnetic, chemical, and bioactive properties that can be used in medical therapy, drug delivery, biosensors, bone replacement, and gas reactors. Their high surface-to-volume ratio also imparts unique catalytic properties. Although nanoparticle synthesis has been performed for centuries [1], perhaps the most well-known form of colloidal Au nanoparticle synthesis used today is the one-pot chemical Turkevich method [2]-[6]. A simple representative balanced aqueous equation for the synthesis for Au seed particles (Au^0: typically 1.5 nm in diameter, and approximately 850 atoms) is presented in Equation (1). This equation depicts the chemical reduction of $HAuCl_4$ to Au^0 using $Na_3C_6H_5O_7$ as the reduction agent.

$$\begin{aligned} &HAuCl_4 \cdot 4H_2O + Na_3C_6H_5O_7 + 18H_2O \\ &\rightarrow Au^0 + H^+ + 3Na^+ + 4Cl^- + 21H_2O + C_6H_5O_7 \cdot H_2O \end{aligned} \tag{1}$$

$$Au^0 \xrightarrow{Na_3C_6H_5O_7} AuNP \tag{2}$$

The growth of Au nanoparticles (AuNP) from an Au^0 seed is given in Equation (2) where the size of the Au nanoparticle depends strongly on the ratio of $Na_3C_6H_5O_7$ to $AuCl_4$. This is because $Na_3C_6H_5O_7$ also acts as a stabilization agent. A typical scenario for this dual process is generally expressed by the following example. At low $Na_3C_6H_5O_7$ concentrations, the growing Au^0 seed particle has a low probability due to low chance of reaction with a $Na_3C_6H_5O_7$ molecule; consequently aggregation occurs resulting in an increase in AuNP size and size distribution, both of which are accompanied by a variety particle morphologies. However, at large $Na_3C_6H_5O_7$ concentrations, the Au^0 seed particles have a high probability of reacting with a $Na_3C_6H_5O_7$ molecule and are quickly stabilized with small spherical diameter and size distribution. In many respects the critical difference in $Na_3C_6H_5O_7$ concentration is a mass transport phenomenon where the supply of $Na_3C_6H_5O_7$ defines the position of the rate-limiting step of Au nanoparticle growth. Naturally, particle growth stops when all the $HAuCl_4$ is consumed in the reaction. Alternatively for Ag nanoparticle synthesis, the Au precursor is normally replaced with silver nitrate ($AgNO_3$) in the presence of a stabilizing agent.

Further development of the one-pot Turkevich method has been to separate the reduction stage from the growth stage using a two-step process that is commonly known as the seed-mediated growth method. In the first step, a reduction agent is used to form Au^0 seeds from the Au precursor. These seeds are then in-

duced to either grow with an anisotropic structure (cube, flower, hexagon, wire, or rod) or as an isotropic sphere by selecting a suitable stabilizer or surfactant agent that caps and protects the nanoparticle. The search for alternative eco-friendly biological reduction agents (bacteria, fungi and algae) is currently being investigated through the twelve principles of Green Chemistry. The first three are: 1) Prevent waste, rather than clean it up. 2) Maximize the use of the materials within the process. 3) Use less and generate less hazardous/toxic material (Grewal *et al.* (2013) [7]). More recently, phytonanotechnology which refers to the use of biochemical molecules (alkaloids, flavonoids, proteins, polysaccharides, cellulose, and phenolic compounds [8]) has been investigated. Plant extract are gaining attention for this application, due to the plentiful supply of cheap raw material, the reduction of toxic waste, and the claimed need for limited purification within the biochemical extraction process prior to the noble metal reduction and stabilizing steps. Keeping within the area of bio-technology, nanoparticles have also been functionalized for biological drug systems (Amina *et al.* (2020) [9]), and nucleic acid delivery systems (Huang *et al.* (2022) [10]). Away from synthesis of nanomaterials, microwave steam generated decontamination of respirator falls into the twelve principles of Green Chemistry (Law *et al.* (2021) [11]).

With Au and Ag nanoparticle expanding applications, it is increasingly highlighted that stringent controls of the synthesis variables (bulk temperature, concentration, pH, solvent medium, and process time) is required. Other non-chemical synthesis routes include: -irradiation [12], photochemical synthesis [13]. However microwave-assisted synthesis [14]-[40] is considered to be a crucial energy source for the Green Chemistry revolution. Therefore a number of microwave-assisted applicators types have been investigated, that comes in the form of mono-mode cavity [14], and turntable loaded multimode applicators [15]-[21], unmodified domestic microwave ovens [22]-[35], temperature controlled microwave chemistry (TCMC) ovens [36]-[40], and axial field helical antenna [41]. The unmodified domestic microwave oven has attracted much interest due to its low cost of ownership and widespread availability for microwave-assisted synthesis of Au nanoparticles [22]-[31], Ag nanoparticles [27] [32]-[40], and Ag substituted hydroxyapatite (AgHA) nanoparticle: the latter being used as bone filler and coatings on metal prosthesis [33].

The investigation highlights above demonstrates how a range of Green Chemistry and non Green Chemistry for microwave-assisted synthesis of Au and Ag nanoparticles, along with AgHa over the last 20 years. For Green Chemistry, one objective has been to replace organic-sodium and organic-bromine with non-toxic reducing agents and stabilization agents, plus replacing solvents such as ethanol with water. The challenge in the latter is the reduction in the polarity index of the solvent (ethanol = 5.2, water = 9 [5]) which plays a critical role in the growth and assembly of the nanoparticle. Given this focus on the chemistry and bio-chemistry aspects of the microwave synthesis, little information has been conveyed regarding the impact of the microwave applicators and their

power source on the synthesis. Indeed in some of the publications, the microwave applicator model has been incorrectly identified [33], unspecified [23] [25] [27] and [31], or the text relating to the duty cycle is ambiguous [24] [34]. To scale-up, or, scale-out, such microwave-assisted synthesis from milligram quantities, a working knowledge of the microwave applicator impact needs be to understand, and the knowledge gained integrated into the already accepted synthesis variables: bulk temperature, concentration, pH, solvent medium, and process time.

The aim of this work is twofold. The first is to apply both quantitative and qualitative analytical tools to investigate historical data within the scientific publications pertaining to microwave-assisted synthesis of Au and Ag nanoparticles. The approach is extended to the microwave applicator types: the domestic multimode microwave oven, commercial multimode microwave digestion applicators, and the axial field helical antenna applicator. All of these applicators are auto-impedance-tuned, and therefore do not require in-depth electrical engineering knowledge to operate them. The second aim is to extract and assemble process energy budget and process energy density data. The more specialized and relatively costly mono-mode applicators that rely on waveguide E- and H-tuning devices and isolators are outside the scope of this work. This work revisits 13 publications pertaining to microwave-assisted synthesis of Au nanoparticles and 16 publications pertaining to the microwave synthesis of Ag nanoparticles; a total of 29 publications. The study is constructed as follows. Section 2 details the reporting of microwave-assisted energy parameter data in the context of the domestic multimode microwave oven, the commercially modified microwave ovens, multimode microwave digesters, and the axial field helical antenna applicator. These applicators may be either operated in the continuous flow (CF), or in the batch mode. In all cases, the microwave power source operates at a frequency of $\lambda_o = 2.45 \pm 0.05$ GHz (~12.2 cm). Section 3 compares their nanoparticle energy phase-space projection with "non-thermal" batch microwave-assisted inactivation of microorganism energy phase-space projections [42]. Section 4 is a summary and outlook of this work. To the aid the reader, the Appendix provides a list of the names of the chemical, biological and plant leaf extracts referred to in this work, along with their common abbreviations, molecular formula, and their general purpose of use.

2. Reporting of Microwave-Assisted Energy Parameter Data

As with all historical datasets collected from different research sources, experimental conditions are not always reported in a consistence manner. This study pulls together the reported microwave parameters, and where necessary clarifies the information using microwave engineering terminology. Given that the sixth principle of Green Chemistry is to minimize electrical energy requirements and operate at ambient room temperature and pressure, the historical data is standardized in terms of power (W, $J \cdot s^{-1}$); process energy budget (kJ); process energy density ($kJ \cdot ml^{-1}$); and bulk temperature (˚C). The collected data is then used to

build a comparative energy phase-space projection [42] [43] of the microwave-assisted synthesis, in terms of Green Chemistry, non Green Chemistry, nanoparticle morphology, and applicator type. Where the published data is insufficient to calculate the standard units of measurement, the outcome of private communication with authors of the original publications is given in the text. Errors in historical reporting of microwave applicators are corrected using online manufacturer's manuals and highlighted with *. Where the microwave parameters are partly reported, this is highlighted with **. Where the microwave applicator is given, but ramp time or duty cycle information is confusing, this is highlighted with ***.

2.1. Domestic Microwave Oven

Today's low cost (typically 60 to 70 euro in 2023) domestic multimode microwave oven has its origins in P.L. Spencer's method of treating foodstuffs, US Patent 2,495,429 (1950) [44]. These ovens are primarily designed to defrost and heat foodstuff using a free-running cavity-magnetron operating at a frequency of f_0 = 2.45 ± 0.05 GHz [45] [46]. In many cases, the cavity-magnetron employs a Feinberg voltage-doubler drive circuit [47] that controls the cavity-magnetron voltage and hence the cavity-magnetron rated instantaneous or continuous wave (CW) output power. For this type of applicator, the cavity-magnetron average output power is normally controlled by a pulse-width-modulation (PWM) circuit that sequentially turns on (T_{on} period) and turns off (T_{off}) the line-voltage at the step-up side of microwave oven transformer (MOT). The result is a time-modulated power waveform that is expressed as a duty cycle, where T_{on} plus T_{off} equals the base-time, and T_{on} minus base-time equals the duty cycle. This is a key aspect of the oven's ability to provide macro control of the dielectric volume heating of foodstuff, or in this case microwave-assisted synthesis of Au and Ag nanoparticles and their functionalization. For example, **Table 1** shows the relationship between T_{on}, T_{off} and base-time and average output power of cavity-magnetron within the Bluesky (model BMG20-8) domestic microwave oven [42].

With reference to **Table 2**: in 2007, Nadagouda *et al.* [22] used an inverter circuit [49] within an unspecified Panasonic microwave oven to reduce $HAuCl_4$ using α-D-glucose ($C_6H_{12}O_6$), maltose, and sucrose ($C_{12}H_{22}O_{11}$). Here the inverter circuit converts the mains supply frequency (50/60 Hz) to a variable rate of some 20 to 45 kHz and by varying this frequency the cavity-magnetron output power is linearly controlled, in this case, 1000 W for 30 and 45 s to achieve the

Table 1. Bluesky microwave oven manufacturer's thermal power specification and acoustic recording timestamp data were obtained for T_{on}, T_{off}, base-time period, and duty cycle.

Bluesky power setting	Measured T_{on} (s)	Measured T_{off} (s)	T_{off} + T_{on} (s)	D (%)
70%, 560 W	~21	~9	30 to 31	~70
55%, 440 W	~16.5	~13	30 to 31	~55
33%, 264 W	~11	~20	30 to 31	~33

Table 2. Microwave oven batch microwave-assisted synthesis of Au nanoparticles. Rows shaded in green highlight Green Chemistry synthesis.

Author	Reduction Method	Metal precursor	Reducing reagent	Power (W) [D %]	Process time (s)	Morphology
Nadagoudà (2007) [22]	One-pot Panasonic Inverter circuit Rated 1 kW	$HAuCl_4 \cdot 4H_2O$	*α*-D-glucose and sucrose Maltose	1000 [100]	30 45	Spherical Cubes, hexagons, prisms
Yazmin (2014) [23]**	One-pot MO unspecified	$HAuCl_4 \cdot 4H_2O$	*Hibiscus rosa-sinensis* leaf extract	420	90	Spherical 16 to 30 nm
Ngo *et al.* (2015) [24]	One-pot Electrolux EMM1908W Rated 700 W	$HAuCl_4 \cdot 4H_2O$	Na_3ct H_2O	210 [30]	600	Spherical 12 to 15 nm
Bhoslae (2015) [25]**	One-pot LG Intellowave, Rated 800 W	$HAuCl_4 \cdot 4H_2O$	DMSO	800 [50]	120 180	Nanoflowers 400 nm Spherical 400 nm
Ngo *et al.* (2016) [26]	One-pot Electrolux EMM1908W Rated 700 W	$HAuCl_4 \cdot 4H_2O$	Na_3ct H_2O	210 [30]	300	Triangle 14 to 22 nm
El-Nagger *et al.* (2016) [27]**	One-pot Galanz (xxx) Rated note given	$HAuCl_4$	Curdlan	Not reported	120 to 600	Au core shell 52 to 54 nm
Shah *et al.* (2019) [28]	Sharp R202ZS Rated 800 W	$HAuCl_4 \cdot 4H_2O$	MPTMS H_2O	800 [100]	60	Hexagonal 100 to 300 nm
Hussein *et al.* (2020) [29]**	Second step MO unspecified	$HAuCl_4 \cdot 4H_2O$	Dextran H_2O	Not reported	40	Spherical ~1 to 2 nm
Putri *et al.* (2021) [30] [48]	One-pot Panasonic NN-SM33HM/W Rated 800 W	$HAuCl_4 \cdot 4H_2O$	White bol guava leaf extract ethanol	800 [100]	120	~17 nm
Diab *et al.* (2022) [31]**	One-pot MO unspecified	$HAuCl_4 \cdot 4H_2O$	CMCT NaOH	Not reported	40	Spherical ~7 nm

target Au nanoparticle. Yasim *et al.* (2014) [23] used an unspecified microwave oven to reduce $HAuCl_4$ with *hibiscus rosa-sinensis* leaf extract within an adjusted 8 ml mixture at 420 W and process time of 90 s to achieve their target AuNP product. Bhosale *et al.* (2015) [25] used an LG intellowave™ sensor microwave oven (model unspecified) to reduce $HAuCl_4$ with Dimethyl sulfoxide (DMSO) for synthesis of nano-flowers and spherical nanoparticles. They used "*360 W, 600 W, and 800 W with on/off mode having time interval of 30 s*". Given this ambiguous text, they found 800 W for 120 s was optimal to produce Au nano-flowers; and 800 W for 180 s was optimal to produce Au spherical nano-

particles. In each case, a 5.5 ml mixture of $HAuCl_4$ and DMSO was used. Publications [27] [29] and [31] originate from the same institutions with related ambiguous reporting of the microwave parameters used. For example, El-Nagger *et al.* (2016) [27] used a Galanz microwave oven, (model number unclear) to reduce a 25 ml mixture of $HAuCl_4$ and bacterial exopolysaccharide (curdlan) with power irradiation time 2 to 10 minutes for an unspecified power level to achieve their Au core shell product. Some four years later, Hussein *et al.* (2002) [29] used an unspecified microwave oven to reduce a 12 ml mixture of $HAuCl_4$ and dextran with an unreported microwave power level for an irradiation time of 40 s to achieve the target AuNP product. Finally, Diab *et al.* (2022) [31] while referencing [27] used an unspecified microwave oven to reduce a 12 ml mixture of $HAuCl_4$ and carboxymethyl chitosan (CMCT) and for an unspecified microwave power level for an irradiation time of 40 s to achieve the target AuNP product. Given the six-year spacing between these publications and the authors' unsuccessful attempts to establish the microwave power conditions these three papers are not explored further.

Table 3 provides the Ag nanoparticles and AgHA synthesis information. Within this group of papers, two publications were found to have ambiguous reporting of microwave variables. First, Saha et al (2013) [32] used an IFB-30SC3 (miss-reported as IFM3SC3) microwave oven to reduce a 60 ml of $AgNO_3$ and *Ocimum* leaf extract using 900 W for 90 s to achieve the target Ag nanoparticles product. Second, Igbal *et al.* (2013) [33] used a Samsung MW71B microwave oven (rated 800 W) to reduce 100 ml of $AgNO_3$ and cetyl-trimethylammonium bromide (CTAB) using a medium high power level (600 W [50]) with a stated 15 s on and

Table 3. Multimode microwave-assisted batch synthesis of Ag nanoparticles and AgHA. Rows shaded in green highlight Green Chemistry synthesis.

Author	Reduction method	Metal precursor	Reducing reagent	Power (W) [D%]	Process time (s)	Morphology
Saha *et al.* (2013) [32]*	One-pot IFB 30SC8 Rated 900 W	$AgNO_3$	*Ocimum* leaf extract	900 [100]	90	Spherical and oval: 3 to 50 nm
Iqbal (2013) [33] [50]	One-pot Samsung MW71B Rated 800 W	$AgNO_3$	$Ca(NO_3)_2{\cdot}4H_2O$ $(NH_4)_2HPO_4$ CTAB	600 [50%]	420	Spherical aggregated ~58 nm
El-Naggar (2016) [27]**	First step Galanz Rated 800 W	$AgNO_3$	Curdlan	Not reported	120	Ag core shell 52 to 54 nm
Jyothi (2020) [34]	One-pot CATA-R Rated 800 W	$AgNO_3$	Coleus amboinicu leaf extract	800 [100]	60	Spherical ~15 nm
Ahmed *et al.* (2021) [35]	One-pot Samsung Rated 800 W	$AgNO_3$	Oxalic acid H_2O CTAB	800 [100]	180	Spherical bimodal ~6.5 and 7.5 nm

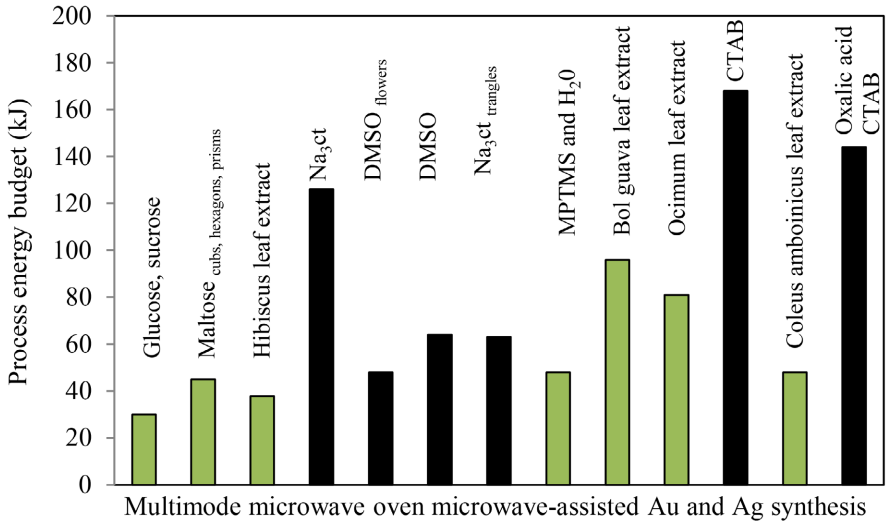

Figure 1. Estimated process energy budget (kJ) to achieve the target NP product within a multimode domestic microwave ovens dataset. The green columns represent Green Chemistry. The black columns represent non-Green Chemistries (Na_3ct, DMSO, and CTAB).

15 s for a processing time of 420 s. However, the stated ON-OFF time equates to a 50% duty cycle or an average power of 400 W of the cavity-magnetron.

The estimated process energy budgets relating to the publications presented in **Table 2** and **Table 3** are given in **Figure 1**. Within this limited dataset it is observed that the Green Chemistry has a lower process energy budget compared to the non Green Chemistry: on average 7.531 kJ against 4.775 kJ. In the specific case of $HAuCl_4$ reduction by *α*-D-glucose ($C_6H_{12}O_6$), sucrose, maltose ($C_{12}H_{22}O_{11}$), hibiscus leaf extract and hydrolyzed 3-Mercaptopropyl trimethoxysilane (MTPMS), the process energy budgets are very similar (30, 48, 48, and 37.8 kJ) indicating that the bio-chemical constituents within the hibiscus extract have a similar reducing efficiency to that of the saccharides. Also not, that the $AgNO_3$ reduction by *Coleus amboinicus* leaf extract shows similar process energy budget to that of the saccharides and hibiscus extract. In contrast the organic-bromine compound within CTAB exhibits the highest process energy budget.

Figure 2 shows the energy phase-space projection of data values from **Figure 1**. In this projection, the process energy budget is plotted on the horizontal-axis over two orders of magnitude (10 to 1000 kJ) and the process energy density is plotted on the vertical-axis over three orders of magnitude (0.1 to 1000 $kJ \cdot m^{-1}$). The log-log axis enables both large and small scale energy processes to be visualized. This also allows a general power-law function ($y = cx^n$, where y and n are constants, with n being referred to as the exponent) to be fitted to a linearized distribution. However, verification of a power-law behavior is not trivial as the linearized data must extend over at least two orders of magnitude on both the x- and y-axis, and yield at good fit at either end of the linearized dataset (Stumpf and Porter (2012) [51]). Using Microsoft Excel linear regression analysis software combined with the Stumpf and Porter criteria, it is observed that all of the Au and Ag nanoparticles data

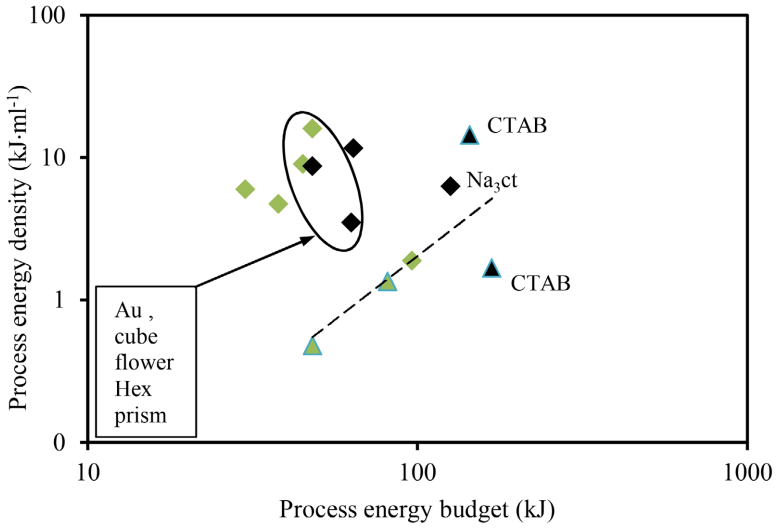

Figure 2. Log-log energy phase-space projection of the target AuNP (diamonds) and AgNP (triangles, dashed trend-line) is presented in **Figure 1**. The green diamonds and triangle represent Green Chemistry. The black diamonds and triangles represent non Green Chemistry.

points form a cluster with center of 76.83 kJ and 6.59 kJ·ml^{-1}. When the data points are separated into Green Chemistry and non Green Chemistry a more detailed picture is formed. That is the non Green Chemistry data points tend to be located at the higher process energy budget range and the Green Chemistry data points tend to be located in the lower energy budget range. An attempt to fit a power-law trend line to AuNP cluster yields a regression analysis of $R^2 = 0.1076$ indicating a poor correlation. Of further note is that the: cube, flower hexagon, prism Au nanoparticles appear to form a sub-cluster within the middle of the Au nanoparticle cluster. Fitting a power-law function to the Ag nanoparticle dataset yields an exponent $n = 1.7874$ over approximately one magnitude on the x- and y-axis with a regression analyses of $R^2 = 0.514$, these two fitting parameters indicate the number of data points is insufficient to detect a power-law relationships.

2.2. Multimode Temperature Control Microwave-Assisted Synthesis

Between 2004 and 2005, Hayes [52], and Hayes and Collins [53] developed the technique of forced air cooling of the outer surface of a vessel containing polar chemicals while administering microwave irradiation, the source of this approach meant it became named as "enhanced microwave synthesis" (EMS). The aim here, is to impart microwave energy directly into the polar molecules, whistle maintaining a relatively low bulk temperature, to induce an increased target product yield by preventing side reactions. In the same time frame the term "non-thermal" and "athermal" microwave-assisted was adopted to highlight a possible difference in the mechanisms involved in microorganism inactivation processes [43] [54]-[59]. The term "temperature controlled microwave chemistry" (TCMC) is also used where the reactants are cooled by refluxing or cooling directly, and where the suspension bulk temperature is monitored and used as

an input parameter of a feedback circuit where the output signal controls the cavity-magnetron power. See for example Kormin *et al.* (2014) [60]. It is noted however that no temperature information was reported in many of the following papers pertaining to TCMC synthesise Ag nanoparticles.

Table 4 lists the microwave parameters of five batch TCMC synthesis of Ag nanoparticles [35] [36] [37] [38] [39]. The first synthesis (Chen *et al.* (2008) [36]) reduced and stabilized AgNO using carboxymethyl cellulose sodium (CMS) within an adjusted 200 ml of H_2O. This one-pot Green Chemistry synthesis takes an unusually long time for a microwave-assisted process to complete (1 to 11 hours). Of further note, this extended process time is comparable to the microwave-assisted extraction of CMS from brewer's spent grain [61]. In 2012, Bahadur *et al.* [37] used a TCMC-064 oven attached with a refluxing system to synthesize $Ag@SiO_2$ Tetraethylorsilicate, (TEOS: $(Si(OC_2H_5)_4)$ as a shell agent plus ethanol (C_2H_5OH). This second step was performed at 360 W for 600 s. However they did not report the quantities of TEOS and C_2H_5OH used. By 2015, Karimipour *et al.* [38] at the University of Rafsanjan, Iran used a similar

Table 4. Multimode temperature controlled microwave-assisted synthesis of AgNP, $Ag@SiO_2$, and $Ag@TiO_2$. Rows shaded in green highlight Green Chemistry synthesis.

Author	Reduction Method	Metal substrate	Reducing, stabilizing, functionalizing agents and solvent	Power (W) [D%]	Process Time (s)	Morphology
Chen (2008) [36]	One-pot TCMC-102 Rated 1 kW	$AgNO_3$	CMS, reducing and stabilizing agent H_2O, solvent	400 [100]	>3600	Spherical ~15 nm
Bahadur (2011) [37]**	Second step Skikoku Keisoku SMW-604 reflux Rated 500 W	AgNP Colloid Spherical 17 nm	TEOS, Si precursor C_2H_6OH, solvent	500 50°C	120	$Ag@SiO_2$ Spherical 20 to 25 nm
Karimipour (2015) [38]	One-pot Shikoku Keisoku SMW-064 reflux Rated 1 kW	$AgNO_3$	DMF, reducing OA, surfactant H_2O, solvent	540 [100]	30	Spherical 10 to 20 nm
Ebrahimi (2016) [39]	One-pot Shikoku Keisoku SMW-064 reflux Rated 1 kW	$AgNO_3$	PVP, stabilizing and capping C_2H_6OH, solvent	360 [100]	60	$Ag@TiO_2$ Spherical ~20 nm
Karimipour (2016) [40]	First step Shikoku Keisoku SMW-064 reflux Rated 1 kW	$AgNO_3$	PVP, capping and stabilizing C_2H_6OH, solvent	360 [100]	60	Spherical ~15 nm
Karimipour (2016) [40]	Second step Shikoku Keisoku SMW-064 reflux Rated 1 kW	PVP-capped AgNP ~15 nm	$Si(OC_2H_5)_4$, silica shell APTES, capping and functionalizing C_2H_6OH, solvent	360 [100]	600	$Ag@SiO_2$ Spherical ~15 nm

TCMC-064 oven attached to a refluxing system to synthesize spherical AgNPs. In this case dimethylformamide (DMF) was used as the reducing agent and oleylamine (OA) as a surfactant and capping agent Using an adjusted 20 ml volume of H_2O. The complete mixture was microwave irradiated as a one-pot synthesis at 540 W for 30 s. In the following year two further papers from the same university and same TCMC attached to a reflux system were published, by Ebrahimi *et al.* (2016) [39], and Karimipour *et al.* (2016) [40]. Ebrahimi *et al.* synthesized Ag@TiO_2 using a one-pot synthesis of $AgNO_3$, PVP in 40 ml of C_2H_5OH with a microwave power of 360 W for 60 s. Whereas Karimipour *et al.* synthesized Ag@SiO_2 core-shells using a two-step process. The first synthesis used water soluble polyvinylpyrrolidone (PVP) and $AgNO_3$ adjusted to 40 ml volume in C_2H_5OH and microwave irradiated at 360 W for 60 s to produce PVP capped Ag nanoparticles. In the second step 100 µl of aminopropyltriethoxysilane (APTES) was added to the 40 ml of PVP capped Ag nanoparticles followed by 1.2 ml of TEOS as the shell agent to produce the target Ag@SiO_2 core shell; the microwave conditions being 360 W for 600 s.

Process Energy Budget and Energy Density Calculations

Using the reported power, process time in Table 4, an estimation of the process energy budgets is given in Figure 3. Here it can be seen the TCMC-102 has a process energy budget (1440 kJ), some 21 times greater than the average energy

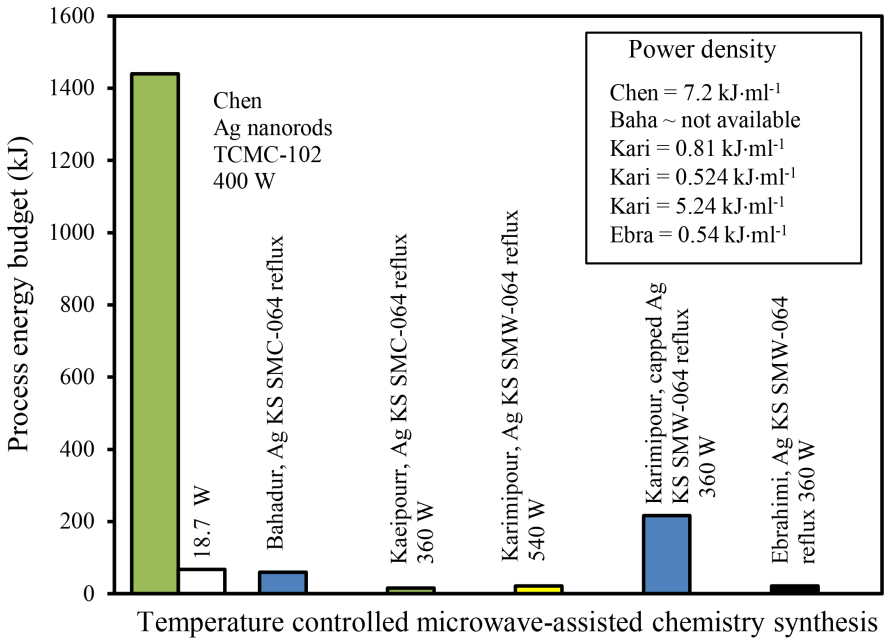

Figure 3. Nanoparticle process energy budget within TCMC ovens: without and with reflux system. Green column represents one-pot Green Chemistry synthesis with a 100% duty cycle. Blue columns represent second step of non Green Chemistry with 100% duty cycle. Yellow column represents the first step non Green Chemistry with 100% duty cycle. Black columns represent one-pot non Green Chemistry with 100% duty cycle. Open column equates to the average process energy budget of the four Shikoku Keisoku SMW-064 process. Insert give the six calculated energy densities.

budget (67.08 kJ) of five Shikoku Keisoku SMW-064 oven experiments. Undoubtedly the high process energy budget is mathematically derived from the extended process time. Nevertheless, given the absence of temperature data, it is interesting to calculate how far TCMC-102 applied power needs fall to average 67.08 kJ. This equates to 18.7 W, and which needs to be accounted for when comparing the two applicator types (TCMC-102 without reflux systems and the Shikoku Keisoku SMW-064 Sk-064 with reflux system).

An estimation of process energy density of five of the TCMC oven synthesis has been calculated using the data within **Figure 3** and their respective mixture quantities (200, 20, 41.2, 41.2 and 40 ml). Bahadur *et al.* [37] is not included due to lack of quantity information. The estimations are found to range between: 7.2, 0.81, 0.524, 5.24, and 0.54 $kJ \cdot ml^{-1}$, respectively. This comparison reveals the energy density disparity between the TCMC-102 and the Shikoku Keisoku SMW-064 with a reflux system is a factor of 2.5. The relative reduction in process energy budget may be due to the ability of the reflux system to maintain the solvents in a similar way to that of microwave-assisted extraction that employs reflux systems [62], in doing so maintaining the rate of Ag reduction. To verify the involvement of these mechanisms further experiments are needed to be undertaken.

2.3. Turntable Loaded Multimode Microwave Digestion Systems

This section looks at five publications pertaining to commercial turntable loaded multimode microwave-assisted synthesis of Au-X and Ag-X nanomaterials, where the microwave applicators are primarily designed for digestion (Bizzi *et al.* (2011) [63]). These microwave digestion systems have been demonstrated to be very effective in the second step synthesis of Ag nano-rods under Na_3ct conditions (Liu *et al.* (2005) [15]), Green Chemistry synthesis of Au-Ag core-shell nanoparticles using $C_6H_{12}O_6$, H_2O and PVP (Blosi *et al.* 2008 [16]), and the non Green Chemistry synthesis of Ag@SnO_2 core-shell (Rai *et al.* (2015) [17]). More recently one-pot synthesis of Ag nanoparticles on graphene sheets has been reported by: Alfano *et al.* (2016) [18], Miglietta *et al.* (2018) [19], and Marinoiu *et al.* (2020) [20]). More recently, a one-pot synthesis of Ag and Ag-Cu nanoparticles using ethylene glycol as the solvent and Copper Acetate ($Cu(CH_3CO)_2$) for the Cu precursor has been reported by Reyes-Blas *et al.* (2020) [21]. However, little information on the suspension quantities was given. Therefore only the process energy budget is calculated, see **Figure 4**.

Generally, these digestion systems (MARS-5, Mars-6, Milestone MicroSYNTH plus (μSYNTH), and the Anton Paar Multiwave (APM)) have a cuboidal multimode cavity that contains a removable turntable that holds a multiple of vessels for single, or, multiple batch processing. Under microwave illumination conditions the rotating turntable smoothes out electromagnetic standing waves and acts as a microwave absorbing dumpy load, in the case of the μSYNTH, a mode stirrer is used to disperse the electromagnetic standing wave [64].

Table 5 lists the reported microwave operating conditions for the five publi

Table 5. Reported turntable loaded multimode microwave-assisted synthesis of AgNPs, Au-Ag core-shells, and Ag decorated graphene sheet.

Author	Reduction method	Metal substrate	Power (W) Temperature (˚C), [D%]	Process time (s)	Morphology
Liu (2005) [15]	Second step MARS-5 Rated 1200 W	$AgNO_3$ Na_3ct A^0 seeds	1200 100˚C [100]	240	Ag rods ~76 nm at 240 s spherical ~57 nm at 480 s
Blosi (2010) [16]	Second step MicroSYNTH plus Rated 2 × 800 W	Au core. $C_6H_{12}O_6$, H_2O, PVP Ag core, $C_6H_{12}O_6$, H_2O, PVP	1600 [75]	300	Spherical Au core-shell ~30 nm Spherical Ag core-shell ~65 nm
Rai (2015) [17]	Second step MARS-5 Rated 1200 W	Ag colloid Na_2SnO_3	1200 70˚C [75]	300 ramp to 70˚C Hold for 36,000	Ag@SnO_2 core-shell 10 - 24 nm
Alfano (2016) [18] Miglietta (2018) [19] [65]	One-pot Anton Paar Multiwave Rated 700 W	$AgNO_3$ Graphene suspension $C_2H_6O_2$	700 [91.67]	120 on 10 off For 45,000	AgNP decorated graphene sheet 2 - 4 nm thick, Semi-spherical AgNP 20 - 30 nm
Marinoiu (2020) [20]	One-pot MARS-6 Rated 1 × 1000 W Rated 1 × 800 W	$HAuCl_4{\cdot}4H_2O$ Graphene oxide $NaBH_4$	800 60˚C 80˚C [100]	1800	AuNP supported on graphene sheet
Reyes-Blas 2020) [21]**	One-pot MARS-6 Rated 1 × 1000 W Rated 1 × 800 W	$AgNO_3$, Cu Acetate Ethylene glycol PVP	1000 155˚C to 180˚C [100]	120	Spherical AgNP ~ 10 nm Irregular Ag-CuNP ~ 15 nm

cations. Briefly the experimental conditions are as follows. Liu *et al.* used 11 ml of reactants within a MARS-5 system with a microwave irradiated 1200 W at 100% duty cycle for a series of process times: 60, 120, 240, and 480 s. After characterization of their rod and spherical Ag nanoparticle products, a process time of 240 s was considered acceptable. Blosi *et al.* used the μSYNTH system that employs two cavity-magnetrons. The power was ramped-up and held, as determined by software that controls the cavity-magnetron pulse width modulated power level for 300 s. The mixture quantity was not given, but the manufactures recommend a value between 10 and 50 ml [64]. Rai *et al.* also used the MARS-5 digestion system with a mixture volume of 21 ml. The applied power is not reported, but it is known that the process involved a ramp time of 5 minutes to reach a bulk temperature of 70˚C and held there for 1 hour, again using PWM of the cavity-magnetron to produce the Ag@SnO_2 core-shell nanoparticles. Alfano *et al.* and Miglietta *et al.* used the APM system, with two aliquots of 3 ml reactant volumes. The applied power was set to 700 W with a 91.67% duty cycle (T_{on} = 120, T_{off} = 10 s) for a process time of 45,000 s to produce AgNP decorated graphene sheets [65]. Finally, Marinoiu *et al.* used the MARS-6 at cavity-magnetron power

of 800 W for a process time of 300 s to produce their target product of Ag nanoparticle supported on a graphene sheet.

Process Energy Budget and Process Energy Density Calculations

Using the reported information within the six publications [15]-[21] and private commutation [65] an estimation of the five synthesis process energy budget has been made with the following duty cycles. For the processes that use a 100%, duty cycle, the applied power is multiplied by the process time [15] [20] and [21]. For the processes that use a 91.67%, duty cycle, the applied multiplied by 91.67% and then multiplied by the process time is used [18] [19] and [65]. For the two processes that use a ramp-time and hold time a best estimation is obtained by multiplying the applied power by 75% then multiplying by the hold process time. The computed values for each synthesis are presented in **Figure 4**. **Figure 5** depicts the computer energy density calculations for references 15 to 20, where the process energy density for [21] is not shown due to insufficient data.

2.4. Axial Field Helical Antenna Applicator

The use of axial field helical antenna applicator entails placing the reactants to be processed within the internal electromagnetic field (reaction zone) of a helical antenna. This type of applicator comprises a solid-state microwave oscillator (λ_o = 2.45 ± 0.05 GHz) and amplifier connected to a 1/4 (or multiple of) wavelength air filled helical antenna without any structural modes (Öhrngren *et al.* (2012) [66]). Under these load conditions the dielectric properties of the reactants will

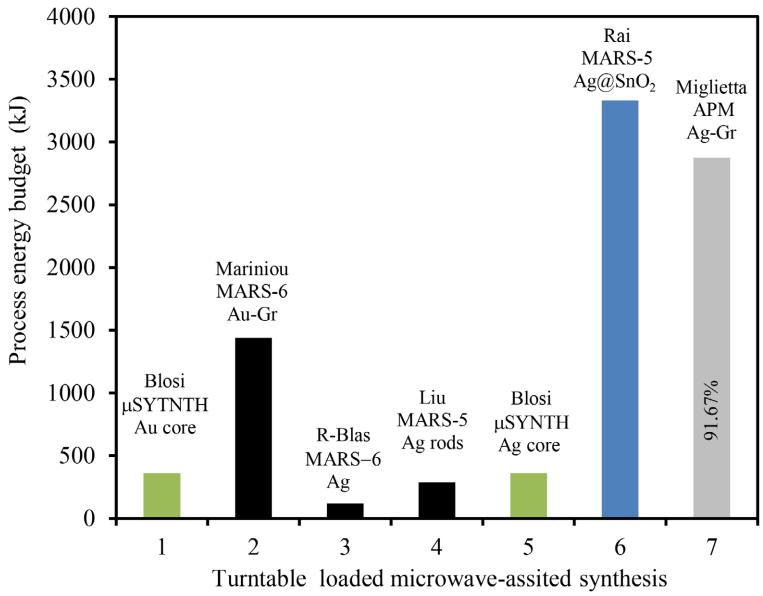

Figure 4. Nanoparticle process energy budget (kJ) within turntable loaded multimode microwave digestion systems. The green columns represent Green Chemistry with 75% duty cycle [16]. The black columns represent non Green Chemistry with a 100% duty cycle [15] [20] and [21]. Blue column represents non Green Chemistry with a 75% duty cycle [17]. Grey column represents non Green Chemistry 91.67% duty cycle [18] [19] and [65].

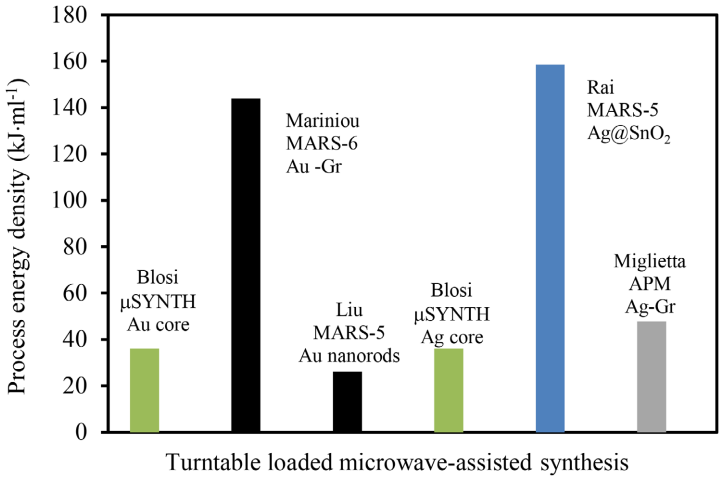

Figure 5. Nanoparticle product process energy density (kJ·ml^{-1}) within turntable loaded multimode microwave digestion systems. The green columns represent Green Chemistry synthesis using 75% duty cycle [16]. Black columns represent non Green Chemistry with 100% duty cycle [15] [20]. Blue columns represent non Green chemistry with 75% duty cycle [17]. Grey column represents non Green Chemistry with 91.67% duty cycle [18] [19] and [65].

reduce the electrical length of helical antenna, thereby frequency-pulling the coupled oscillator. As long as the degree of pulling is within the oscillator −3 dB bandwidth, which depends on the coupling factor between the oscillator and antenna (Law (2008) [67], Amry, Law and Boyd (2012) [68]) power is maintained to the antenna. In effect the applicator has an auto impedance matching circuit, similar to the cavity-magnetron waveguide bandwidth of a domestic microwave oven (Law and Dowling (2021) [46]).

In 2016, Bayazit *et al.* [41]) reported on a one-pot constant flow microwave-assisted anisotropic growth of Au nanowires and rods. In this synthesis, $HAuCl_4{\cdot}4H_2O$ is reduced using Na_3ct, The synthesis apparatus comprise the commercial Discover 2 (CEM Microwave Technology Ltd), applicator within which is placed a coiled flow reactor constructed from approximately 6 ml volume of 3.4 mm outer diameter Teflon tubing. Using this diameter tubing, the microwave penetration depth is > the tubing diameter (Ye *et al.* (2020) [69]) thereby assuring uniform dielectric heating whilst providing minimal disturbance of the antenna electric field. Finally, the reactants are forced through the reactor using a syringe pump at a rate of 4, 7, and 10 ml·min^{-1} that equated to a residence time (τ) between 1.5, 0.85, and 0.6 minutes. The residence time (τ) is calculated using Equation (3).

$$\tau = \frac{\text{volume}}{\text{flow rate}}, \text{ where time is measured in minutes} \quad (3)$$

The residence time measured in seconds multiple by the applied microwave power equates to the process energy budget. For reproducible anisotropic growth of Au nano-rods with an aspect ratio (length × width) of approximately ~10 × 7 nm, the power, flow rate and residence time are presented in **Table 6**.

Process Energy Budget Calculations

Using the same energy calculation methodology as in 3.1, and converting minutes to seconds a process energy budget of 3.2 kJ and energy density of 0.81 $kJ \cdot ml^{-1}$ is obtained. This equates to an energy transfer efficiency of 0.253 $kJ \cdot ml^{-1}$ per applied kJ at 36 W applied power.

2.5. Energy Phase-Space Projection of TCMC, Digester and Axial Field Helical Antenna Applicators

This section describes energy phase-space projection mapping and comparison of the microwave energy parameters obtained for the four microwave applicators types and their NP synthesis. The results of the computation are given over four orders of magnitude on both the horizontal x-axis (1 to 10,000 kJ) and the vertical y-axis (0.1 to 100 $kJ \cdot ml^{-1}$) Figure 6. The figure reveals a number of identifiable features within the datasets.

Firstly, the mapping process reveals that the axial field helical field antenna applicator (star) exhibits the least energy density (3.2 kJ, 0.81 $kJ \cdot m^{-1}$; at an

Table 6. Axial field helical antenna microwave-assisted synthesis of Au nano-rods.

Author	Microwave applicator	Metal substrate	Reducing reagent	Power (W)	Flow rate ($ml \cdot min^{-1}$) [τ = min]	Morphology
Bayazit (2016) [41]	Discover 2 CEM corporation	$HAuCl_4 \cdot 4H_2O$	Na_3ct H_2O	36	4 [1.5]	Au nano-rods (length × width) ~ 10 × 7 nm

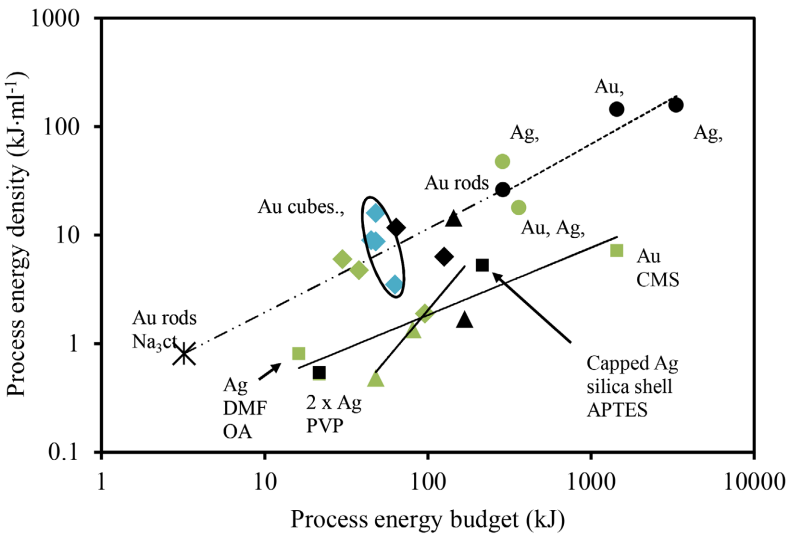

Figure 6. Log-log energy phase-space projection of Green Chemistry (Green) and non Green Chemistry (black) for the axial field helical antenna system (star), TCMC systems (squares, power-law dashed trend-line), and turntable loaded digestion systems (circles, power-law dotted trend-line, with the three large squares representing a 75% duty cycle). duty cycle. The four blue diamond's represent the Au crystal morphology cluster as first shown in Figure 2.

applied power of 36 W). Followed by microwave oven (76.83 ± 39 kJ and 4.47 ± 3.9 kJ·ml^{-1}), TCMC (343 ± 321.5 kJ, and 2.86 ± 2.3 kJ·m^{-1}), digester systems (1010 ± 620 kJ, and 36.2 ± 50.7 kJ·m^{-1}). In the case of the axial field helical antenna applicator data point, this is clearly separated from the nearest TCMC data points indicating the log-log scale is still enabling small and large values to be visualized.

Secondly, a power-law fitted through the digester (circles) and TCMC (squares) datasets provide a local (<two orders of magnitude) exponent n = 0.8412 and 0.6199, and regression analyses of R^2 = 0.7642 and 0.8974, respectively. In addition the digester dataset power-law trend-line (by eye) projects back from the Au nano-rod data point, through the microwave oven crystal morphology cluster and on to the axial field helical antenna Au nano-rod data point (3.2 kJ and 0.8 kJ·m^{-1}). This projection is quantified by a power-law fit over two orders of magnitude (dash-dash trend-line) with an exponent n = 0.7719, and regression analyses R^2 = 1. When the digester, microwave oven and axial field helical antenna exponent n values are averaged, an exponent n = 0.806 is obtained. In comparison the exponent n = 0.699 TCMC dataset is offset by some −10 kJ·ml^{-1} to the digester-to-axial field helical antenna power-law trend-line, indicating there is an additional mechanism involved. Finally, Au and Ag microwave-assisted synthesis exponent may be derived by averaging all exponents which equate to n = 0.730 ± 0.07.

Thirdly, the Au and AgNP morphology outcomes within their respective applicator type reveal a degree of correlation. For example, the constant flow axial field helical antenna applicator (star) that uses the non Green Chemistry Na_3ct reducing agent yields the lowest process energy budget and process energy density for all the datasets reported in this study. The five TCMC data points representing spherical and core shell Ag nanoparticles have the second least energy efficiency for both Green Chemistry and Non Green Chemistry. The digester dataset has the lest energy efficiency performance, but this may be due to the estimated 75% duty cycle used to characterize the ramp and hold-time power levels.

Fourthly, assuming a microwave-assisted nanoparticle synthesis power-law exponent n = 0.730 ± 0.07 reflects the historical nanoparticle datasets. It is reasonable to assume that the relative phase-space location of a given target Au, or, Ag nanoparticles and their yield (counts per ml) along this exponent will be altered by an informed change the in synthesis variables: bulk temperature, concentration, pH, solvent medium, and process time, or purification of plant extract suspension (thereby removing potential side reactions) prior to the nanoparticle synthesis step.

3. Energy Phase-Space Projection with Microwave-Assisted Processes

This section describes the use of the energy phase-space projection to compare data reported in *"Revisiting 'non-thermal' batch microwave oven inactivation of*

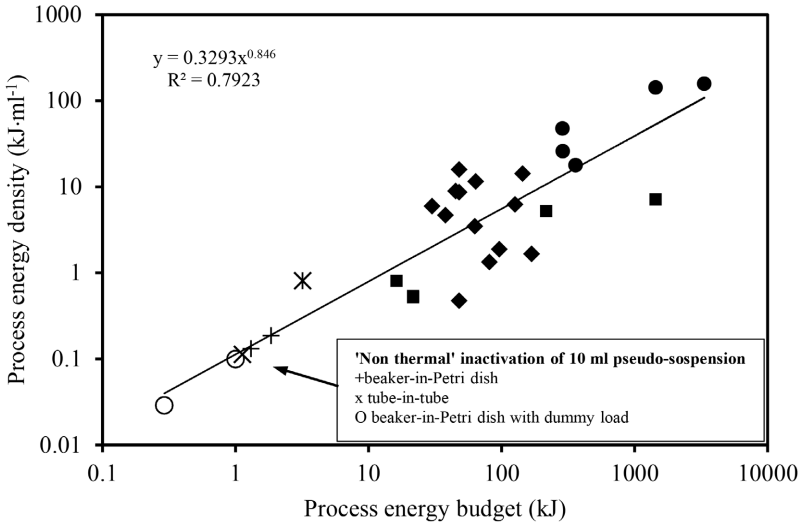

Figure 7. Log-log energy phase-space projection of Au and Ag Green Chemistry and non Green Chemistry for the axial field helical antenna system (star), TCMC systems (black square), turntable loaded digestion systems (black circle), and microwave oven (black diamond), and "non thermal" inactivation of microorganisms within microwave ovens (plus sign, star and open circles [42]).

microorganisms, American Journal of Analytical Chemistry, 14(1), 28-54, (2023)" [42] with Green Chemistry and non Green Chemistry outcomes as presented in **Figure 6**. The result of this comparison is given in **Figure 7**: with a horizontal-axis of 0.1 to 10,000 kJ, and a vertical-axis of 0.1 to 1000 kJ·m^{-1}. The "non thermal" microwave-assisted data is generated within a Bluesky (model BMG20-8) domestic microwave oven using 55%, duty cycle (440 W of 800 W) for 10 ml pseudo-suspension (water) within different Pyrex glass containers (beaker-in-Petri dish (+), tube-in-tube (X), and beaker-in-Petri dish plus dummy load (O) that are simultaneously cooled by an ice or ice slurry bath. The experiments were designed mimic bacteriophage and *E. coil* ≥ 4 $\log_{10}$ inactivation reported by [54]-[58].

The comparative mapping reveals that the "non-thermal" microwave-assisted pseudo-suspension inactivation experimental data points (plus sign, cross, and open circles) are aligned to all the Green Chemistry and non Green Chemistry Au and Ag nanoparticle synthesis datasets across all four applicator types. A power-law fit to all datasets yield a "global" first-order kinetics "non-thermal" and thermal microwave-assisted exponent n = 0.846 (R^2 = 0.7923) over four magnitudes and all four applicator types.

4. Summary

This study has examined 29 papers pertaining to microwave-assisted synthesis of Au and Ag nanoparticles. Within this group of papers, 28 nanoparticle synthesis routes have been analyzed for their process energy budget (kJ) and process energy density (kJ·ml^{-1}) as function of four microwave applicator types: domestic microwave oven, TCMC oven, digester, and axial field helical antenna. Both

Green Chemistry and non Green Chemistry is also been considered. A log-log energy phase-space projection where the process energy budget is plotted on the horizontal axis and process energy density is plotted on the vertical axis for the visualization of the synthesis. Using this projection format, the data distribution is linearization over three orders of magnitude on both vertical and horizontal axis, resulting in a first-order power-law relationship with an exponent of n.

Allowing for the inconsistencies in the historical reporting of microwave power and process time variables, 28 Au and Ag nanoparticle microwave-assisted synthesis processes yield an average first-order power-law exponent of $n = 0.730 \pm .0.07$. Within the dataset, the axial field helical field antenna applicator (Discover 2) is found to be the most energy efficient (0.253 $kJ \cdot m^{-1}$ per applied kJ, at 36 W). This is followed by the unmodified domestic microwave oven (4.47 ± 3.9 $kJ \cdot ml^{-1}$ per 76.83 ± 39 kJ), then TCMC ovens (2.86 ± 2.3 $kJ \cdot m^{-1}$ per 343 ± 321.5 kJ), and the digester applicator dataset being the least energy efficient (36.2 ± 50.7 $kJ \cdot m^{-1}$ per 1010 ± 620 kJ). In addition, a comparison with reconstructed "non-thermal" microwave oven inactivation microorganism experiments, yields a power-law signature of $n = 0.846$ ($R^2 = 0.7923$) over four orders of magnitude.

It is found that the anisotropic nanoparticle morphology growth occurs in the axial field helical antenna and in some unmodified domestic microwave ovens. It is proposed that the relative phase-space location of the anisotropic nanoparticles is not fixed, but reflects the specific historical experimental variables (bulk temperature, concentration, pH, solvent medium, and process time). In the case of the TCMC oven dataset, it is observed that spherical and metal core shell nanoparticles are grown. It is also noted that the use of a reflux system significantly reduces the process energy budget requirement. This characteristic generates a phase transition within the power-law signature.

As regards to Green Chemistry versus non Green Chemistry synthesis. This study highlights that organic-brome and organic-sodium containing reduction agents exhibit the highest process energy budgets when used in a domestic microwave oven applicator. Saccharides and plant extracts that contain an assortment of biochemical molecules (alkaloids, flavonoids, proteins, polysaccharides, cellulose, and phenolic compounds) were found to have the lowest process energy budgets. It is noted that the Bio-chemistry (bacterial exopolysaccharide and plant extracts) reduction agents were not purified prior to the nanoparticle synthesis. This non-purification aspect needs further investigation with the aim of removing side-reactions, and increasing product yield, both of which are likely to be reflected in lower process energy budgets and higher microwave conversion efficiency ($kJ.ml^{-1}$ per applied kJ).

This study contributes to the understanding of microwave-assisted synthesis of Au and Ag nanoparticle by using energy phase-space projections. With regard to the outlook of this study, the analytical approach taken here may be employed in the design and debugging of future microwave-assisted Au and Ag nanoparticle synthesis. The linear regression analysis used to estimate the power-law

signature assumes that outlier data points > 100 kJ influence the value of n. Nevertheless, keeping to one power-law model, it is proposed that researchers can develop specific recipe short-loop experimental iteration cycles where the feedback information builds a data-rich energy phase-space projection, for target product innovation. It is also proposed that this visual and analytical approach may be extended to microwave-assisted synthesis of different nanoparticles containing other noble and transition metals.

Acknowledgements

The authors would like to thank: Dr. S.E. Putri (Universitas Negeri Makassar, Indonesia) and Prof. M. L. Miglietta (ENEA C.R. Portici, P.le E. Fermi 1, Portici, I-80055 Naples, Italy) for allowing us to use their unpublished experimental data.

Conflicts of Interest

The authors declare no conflicts of interest regarding the publication of this paper.

References

[1] Bayda, S., Adeel, M., Tuccinardi, T., Cordani, M. and Rizzolio, F. (2020) The History of Nanoscience and Nanotechnology: From Chemical-Physical Applications to Nanomedicine. *Molecules*, **25**, Article 112. https://doi.org/10.3390/molecules25010112

[2] Turkevich, J., Stevenson, P.C. and Hillier, J. (1951) A Study of the Nucleation and Growth Processes in the Synthesis of Colloidal Gold. *Discussions of the Faraday Society*, **11**, 55-75. https://doi.org/10.1039/df9511100055

[3] Ngo, V.K.T., Huynh, T.P., Nguyen, D.G., Nguyen, H.P.U., Lam, Q.V. and Huynh, T.D. (2015) Synthesis and Spectroscopic Characterization of Gold Nanobipyramids Prepared by a Chemical Reduction Method. *Advances in Natural Sciences: Nanoscience and Nanotechnology*, **6**, Article 045017. https://doi.org/10.1088/2043-6262/6/4/045017

[4] Jurkin, T., Guliš, M., Dražić, G. and Gotić, M. (2016) Synthesis of Gold Nanoparticles under Highly Oxidizing Conditions. *Gold Bulletin*, **49**, 21-33. https://doi.org/10.1007/s13404-016-0179-3

[5] Hussain, M.H., Bakar, N.F.A., Mustapa, A.N., Low, K.F., Othman, N.H. and Adam, F. (2020) Synthesis of Varies Size Gold Particles by Chemical Reduction Method with Different Solvents. *Nanoscale Research Letters*, **15**, Article No. 140. https://doi.org/10.1186/s11671-020-03370-5

[6] Dong, J., Carpinone, P.L., Pyrgiotakis, G., Demokritou, P. and Moudgil, B.M. (2020) Synthesis of Precision Gold Nanoparticles Using Turkevich Method. *KONA Powder and Particle Journal*, **37**, 224-232. https://doi.org/10.14356/kona.2020011

[7] Grewal, A.S., Kumar, K., Redhu, S. and Bhardwaj, S. (2013) Microwave Assisted Synthesis: A Green Synthesis Chemistry Approach. *International Research Journal of Pharmaceutical and Applied Sciences*, **3**, 278-285.

[8] Bharadwaj, K.K., Rabha, B., Pati, S., Sarkar, T., Choudhury, B.K., Barman, A., Bhattacharjya, D., Srivastava, A., aishya, D., Edinur, B.H.A., Kari, Z.A. and Noor, N.H.M. (2021) Green Synthesis of Gold Nanoparticles Using Plant Extracts as

Beneficial Prospect for Cancer Theranostics. *Molecules*, **26**, Article 6389. https://doi.org/10.3390/molecules26216389

[9] Amina, S.J. and Guo, B. (2020) A Review on the Synthesis and Functionalization of Gold Nanoparticles as a Drug Delivery Vehicle. *International Journal of Nanomedicine*, **15**, 9823-9857. https://doi.org/10.2147/IJN.S279094

[10] Huang, M., Xiong, E., Wang, Y., Hu, M., Yue, H., Tian, T., Zhu, D., Liu, H. and Zhou, X. (2022) Fast Microwave Heating-Based One-Step Synthesis of DNA and RNA Modified Gold Nanoparticles. *Nature Communications*, **13**, Article No. 968. https://doi.org/10.1038/s41467-022-28627-8

[11] Law, V.J. and Dowling, D.P. (2021) MGS Decontamination of Respirators: A Thermodynamic Analysis. *Global Journal of Research in Engineering and Computer Science*, **1**, 1-17.

[12] Li, T., Park, H.G. and Choi, S.H. (2007) γ-Irradiation-Induced Preparation of Ag and Au Nanoparticles and Their Characterizations. *Materials Chemistry and Physics*, **105**, 325-350. https://doi.org/10.1016/j.matchemphys.2007.04.069

[13] Shiraishi, Y., Tanaka, H., Sakamoto, H., Ichikawa, S. and Hiraia, T. (2017) Photoreductive Synthesis of Monodispersed Au Nanoparticles with Citric Acid as Reductant and Surface Stabilizing Reagent. *The Royal Society of Chemistry Advances*, **7**, 6187-6192. https://doi.org/10.1039/C6RA27771C

[14] Sommer, W.J. and Weck, M. (2007) Facile Functionalization of Gold Nanoparticles via Microwave-Assisted 1,3 Dipolar Cycloaddition. *Langmuir*, **23**, 11991-11995. https://doi.org/10.1021/la7018742

[15] Liu, F.K., Huang, P.W., Chang, Y.C., Ko, C.J., Ko, F.H. and Chu, T.C. (2005) Formation of Silver Nanorods by Microwave Heating in the Presence of Gold Seeds. *Journal of Crystal Growth*, **273**, 439-445. https://doi.org/10.1016/j.jcrysgro.2004.09.043

[16] Blosi, M., Albonetti, S., Gatti, F., Dondi, M., Migliori, A., Ortolani, L., Morandi, V. and Baldi, G. (2010) Au, Ag and Au-Ag Nanoparticles: Microwave-Assisted Synthesis in Water and Applications in Ceramic and Catalysis. *Nanotechnology*, **1**, 352-355.

[17] Rai, P., Majhi, S.M., Yu, Y.T. and Lee, J.H. (2015) Synthesis of Plasmonic Ag@SnO_2 Core–Shell Nanoreactors for Xylene Detection. *Royal Society of Chemistry*, **5**, 17653-17659. https://doi.org/10.1039/C4RA13971B

[18] Alfano, B., Polichetti, T., Mauriello, M., Miglietta, M.L., Ricciardella, F., Massera, E. and Francia, G.D. (2016) Modulating the Sensing Properties of Graphene through an Eco-Friendly Metal-Decoration Process. *Sensors and Actuators B*: *Chemical*, **222**, 1032-1042. https://doi.org/10.1016/j.snb.2015.09.008

[19] Miglietta, M.L., Alfano, B., Polichetti, T., Massera, E., Schiattarella, C. and Francia, G.D. (2018) Effective Tuning of Silver Decorated Graphene Sensing Properties by Adjusting the Ag NPs Coverage Density. *Sensors*: *Proceedings of the Third National Conference on Sensors*, Rome, 23-25 February 2016, 82-89. https://doi.org/10.1007/978-3-319-55077-0_11

[20] Marinoiu, A., Andrei, R., Vagner, I., Niculescu, V., Bucra, F., Constantinescu, M. and Carcadea, E. (2020) One Step Synthesis of Au Nanoparticles Supported on Graphene Oxide Using an Eco-Friendly Microwave-Assisted Process. *Materials Science*, **26**, 249-254. https://doi.org/10.5755/j01.ms.26.3.21857

[21] Reyes-Blas, M., Maldonado-Luna, N.M., Rivera-Quiñones, C.M., Vega-Avila1, A.L., Roman-Velázquez, F.R. and Perales-Perez, O.J. (2020) Single Step Microwave Assisted Synthesis and Antimicrobial Activity of Silver, Copper and Silver-Copper

Nanoparticles. *Journal of Materials Science and Chemical Engineering*, **8**, 13-29. https://doi.org/10.4236/msce.2020.88002

[22] Nadagouda, M.N. and Varma, R.S. (2008) Microwave-Assisted Shape-Controlled Bulk Synthesis of Noble Nanocrystals and Their Catalytic Properties. *Crystal Growth & Design*, **8**, 291-295.

[23] Yasmin, A., Ramesh, K. and Rajeshkumar, S. (2014) Optimization and Stabilization of Gold Nanoparticles by Using Herbal Plant Extract with Microwave Heating. *Nano Convergence*, **1**, Article No. 12. https://doi.org/10.1186/s40580-014-0012-8

[24] Ngo, V.K.T., Nguyen, H.P.U., Huynh, T.P., Tran, N.N.P., Lam, Q.V. and Huynh, T.D. (2015) Preparation of Gold Nanoparticles by Microwave Heating and Application of Spectroscopy to Study Conjugate of Gold Nanoparticles with Antibody *Escherichia coli* O157:H7. *Advances in Natural Sciences*: *Nanoscience and Nanotechnology*, **6**, Article 035015. https://doi.org/10.1088/2043-6262/6/3/035015

[25] Bhosale, M.A., Chenna, D.R., Ahire, J.P. and Bhanage, B.M. (2015) Morphological Study of Microwave-Assisted Facile Synthesis of Gold Nanoflowers/Nanoparticles in Aqueous Medium and Their Catalytic Application for Reduction of p-Nitrophenol to p-Aminophenol. *Royal Society of Chemistry Advances*, **5**, 52817-52823. https://doi.org/10.1039/C5RA05731K

[26] Ngo, V.K.T., Nguyen, H.P.U., Huynh, T.P. and Lam, Q.V. (2016) A Low Cost Technique for Synthesis of Gold Nanoparticles Using Microwave Heating and Its Application in Signal Amplification for Detecting *Escherichia coli* O157:H7 Bacteria. *Advances in Natural Sciences*: *Nanoscience and Nanotechnology*, **7**, Article 035016. https://doi.org/10.1088/2043-6262/7/3/035016

[27] El-Naggar, M.E., Shaheen, T.I., Fouda, M.M.G. and Hebeish, A.A. (2016) Eco-Friendly Microwave-Assisted Green and Rapid Synthesis of Well-Stabilized Gold and Core-Shell Silver-Gold Nanoparticles. *Carbohydrate Polyme*, **20**, 1128-1136. https://doi.org/10.1016/j.carbpol.2015.10.003

[28] Shah, K.W. and Zheng, L. (2019) Microwave-Assisted Synthesis of Hexagonal Gold Nanoparticles Reduced by Organosilane (3-Mercaptopropyl) Trimethoxysilane. *Materials*, **12**, Article 1680. https://doi.org/10.3390/ma12101680

[29] Hussein, J., El-Naggar, M.E., Fouda, M.M.G., Othman, S.I., Allam, A.A., Nadwa, E.H., Rashwan, E.K. and Hendawy, O.M. (2020) Eco-Friendly Microwave Synthesis of Gold Nanoparticles for Attenuation of Brain Dysfunction in Diabetic Rats. *Journal of Cluster Science*, **32**, 423-435. https://doi.org/10.1007/s10876-020-01801-y

[30] Putri, S.E., Pratiwi, D.E., and Side, S. (2021) The Effect of Microwave Irradiation on Synthesis of Gold Nanoparticles Using Ethanol Extract of White Bol Guava Leaves. *Journal of Physics: Conference Series*, **1752**, Article 012058. https://doi.org/10.1088/1742-6596/1752/1/012058

[31] Diab, S.F.H., Sharaby, C.M., Elsayed, H.H., Roushdy, M.M. and Fouda, M.M.G. (2022) Hyaluronic Acid/Carboxymethyl Chitosan Embedded Gold Nanoparticles Modulate High Fructose Diet Induced Diabetes Changes in Rat. *Egyptian Journal of Chemistry*, **65**, 183-193.

[32] Saha, S., Malik, M.M. and Qureshi, M.S. (2013) Microwave Synthesis of Silver Nano particles. *Nano Hybrids*, **4**, 99-112. https://doi.org/10.4028/www.scientific.net/NH.4.99

[33] Iqbal, N., Kadir, M.R.A., Malek, N.A.N.N., Mahmood, N.H.B., Murali, M.R. and Kamarul, T. (2013) Characterization and Antibacterial Properties of Stable Silver Substituted Hydroxyapatite Nanoparticles Synthesized through Surfactant Assisted Microwave Process. *Materials Research Bulletin*, **48**, 3172-3177.

https://doi.org/10.1016/j.materresbull.2013.04.068

[34] Jyothi, D., Cherriyan, S.P., Ahmed, S.R.R., Priya, S., James, J.P. and T.G.P. (2020) Microwave Assisted Green Synthesis of Silver Nanoparticles Using Coleus Amboinicus Leaf Extract. *International Journal of Applied Pharmaceutics*, **12**, 56-61. https://doi.org/10.22159/ijap.2020v12i3.37121

[35] Ahmed, F., AlOmar, S.Y., Albalawi, F., Arshi, N., Dwivedi, S., Kumar, S., Shaalan, N.M. and Ahmad, N. (2021) Microwave Mediated Fast Synthesis of Silver Nanoparticles and Investigation of Their Antibacterial Activities for Gram-Positive and Gram-Negative Microorganisms. *Crystals*, **11**, Article 666. https://doi.org/10.3390/cryst11060666

[36] Chen, J., Wang, J., Zhang, X. and Jin, Y. (2008) Microwave-Assisted Green Synthesis of Silver Nanoparticles by Carboxymethyl Cellulose Sodium and Silver Nitrate. *Materials Chemistry and Physics*, **108**, 421-424. https://doi.org/10.1016/j.matchemphys.2007.10.019

[37] Bahadur, N.M., Furusawa, T., Sato, M., Kurayama, F., Siddiquey, I.A. and Suzuki, N. (2011) Fast and Facile Synthesis of Silica Coated Silver Nanoparticles by Microwave Irradiation. *Journal of Colloid and Interface Science*, **355**, 312–320. https://doi.org/10.1016/j.jcis.2010.12.016

[38] Karimipour, M., Shabani, E. and Molaei, M. (2015) Microwave Synthesis of Oleylamine-Capped Ag Nanoparticles in Aqueous Solution. *Materials Science*, **21**,182-186. https://doi.org/10.5755/j01.ms.21.2.6480

[39] Ebrahimi, M., Zakery, A., Karimipour, M. and Molaei, M. (2016) Nonlinear Optical Properties and Optical Limiting Measurements of Graphene Oxide Ag@TiO_2 Compounds. *Optical Materials,* **57**, 146-152. https://doi.org/10.1016/j.optmat.2016.04.039

[40] Karimipour, M., Mostoufirad, S., Molaei, M., Nikabadi, H.R. and Nesheli, A.G. (2016) Free Reducing Agent, One Pot, and Two Steps Synthesis of Ag@SiO_2 Core-Shells Using Microwave Irradiation. *Journal of Nano- and Electronic Physics*, **8**, 03020.

[41] Bayazit, M.K., Yue, J., Cao, E., Gavriilidis, A. and Tang, J. (2016) Controllable Synthesis of Gold Nanoparticles in Aqueous Solution by Microwave Assisted Flow Chemistry. *ACS Sustainable Chemistry & Engineering*, **4**, 6435-6442. https://doi.org/10.1021/acssuschemeng.6b01149

[42] Law, V.J. and Dowling, D.P. (2023) Revisiting "Non-Thermal" Batch Microwave Oven Inactivation of Microorganisms. *American Journal of Analytical Chemistry*, **14**, 28-54. https://doi.org/10.4236/ajac.2023.141003

[43] Law, V.J. and Dowling, D.P. (2022) Microwave-Assisted Inactivation of Fomite-Microorganism Systems: Energy Phase-Space Projection. *American Journal Analytical Chemistry*, **13**, 255-276. https://doi.org/10.4236/ajac.2022.137018

[44] Spencer, P.L. (1950) Method of Treating Foodstuffs. US Patent No. 2495429.

[45] Vollmer, M. (2004) Physics of the Microwave Oven. *Physics Education*, **39**, 74-81. https://doi.org/10.1088/0031-9120/39/1/006

[46] Law, V.J. and Dowling, D.P. (2019) Microwave Oven Plasma Reactor Moding and Its Detection. In: Skiadas, C.H. and Dimotikalis, Y., Eds., 12*th Chaotic Modeling and Simulation International Conference*, *Springer Proceedings in Complexity*, Springer, Cham, 157-179. https://doi.org/10.1007/978-3-030-39515-5_14

[47] Feinberg, A.E. (1968) Power Supply Circuit for Continuous Wave Magnetron Operated by Pulse Direct Current. US Patent No. 3396342.

[48] Putri, S.E. (2023) Private Communication via ResearchGate Regarding Type of Microwave Oven and Process Conditions Used.

[49] Min, G.I., Han, S.J. and Shin, D.M. (2005) Inverter Circuit of Microwave Oven. US Patent No. 6936803B2.

[50] Samsung M71B Owner's Instructions and Cooking Guide. https://www.manualslib.com/manual/2249998/Samsung-Mw71b.html

[51] Stumpf, M.P.H. and Porter, M.A. (2012) Critical Truths about Power Laws. *Science*, **355**, 665-666. https://doi.org/10.1126/science.1216142

[52] Hayes, B.L. (2004) Recent Advances in Microwave-Assisted Synthesis. *Aldrichimica Acta*, **73**, 66-77.

[53] Hayes, B.L. and Collins, M.J. (2005) Reaction and Temperature Control for High Power Microwave-Assisted Chemistry Techniques. US Patent No. 6917023.

[54] Wang, A., Cheng, N., Liou, Y.T. and Lin, K. (2001) Inactivation of Bacteriophage by Microwave Irradiation. *Journal of Experimental Microbiology and Immunology*, **1**, 9-18.

[55] Asay, B., Tebaykina, Z., Vlasova, A. and Wen, M. (2008) Membrane Composition as a Factor in Susceptibility of *Escherichia coli* C29 to Thermal and Non-Thermal Microwave Radiation. *Journal of Experimental Microbiology and Immunology*, **12**, 7-13.

[56] Baines, B. (2005) A Comparison of the Effects of Microwave Irradiation and Heat Treatment of T4 and T7 Bacteriophage. *Journal of Experimental Microbiology and Immunology*, **7**, 57-61.

[57] Bryant, S., Rahmanian, R., Tam, H. and Zabetian, S. (2007) Effects of Microwave Irradiation and Heat on T4 Bacteriophage Inactivation. *Journal of Experimental Microbiology and Immunology*, **11**, 66-72.

[58] Barnett, C., Huerta-Mounoz, U., James, R. and Pauls, G. (2006) The Use of Microwave Radiation in Combination with EDTA as an Outer Membrane Disruption Technique to Preserve Metalloenzyme Activity in *Escherichia coli*. *Journal of Experimental Microbiology and Immunology*, **9**, 1-5.

[59] Horikoshi, S., Tsuzuki, J., Kajitani, M., Abec, M. and Serpone, N. (2008) Microwave-Enhanced Radical Reactions at Ambient Temperature Part 3: Highly Selective Radical Synthesis of 3-Cyclohexyl-1-Phenyl-1-Butanone in a Microwave Double Cylindrical Cooled Reactor. *New Journal of Chemistry*, **32**, 2257-2262.

[60] Kormin, F., Nour, A.H., Yunus, R.M., Rivai, M. and Kormin, S. (2014) Performance of Temperature Control Microwave Closed System (TCMCS). *International Journal of Engineering Sciences & Research Technology*, **3**, 135-142.

[61] Santos, D.M.D., Bukzem, A.D.L., Ascheri, D.P.R., Signini, R. and Aquino, G.L.B.D. (2015) Microwave-Assisted Carboxymethylation of Cellulose Extracted from Brewer's Spent Grain. *Carbohydrate Polymers*, **131**, 125-133. https://doi.org/10.1016/j.carbpol.2015.05.051

[62] Akhtar, I., Javad, S., Yousaf, Z., Iqbal, S. and Jabeen, K. (2019) Microwave Assisted Extraction of Phytochemicals an Efficient and Modern Approach for Botanicals and Pharmaceuticals. *Pakistan Journal of Pharmaceutical Sciences*, **32**, 223-230.

[63] Bizzi, C.A., Flores, E.M., Barin, J.S., Garcia, E.E. and Nóbrega, J.A. (2011) Understanding the Process of Microwave-Assisted Digestion Combining Diluted Nitric acid and Oxygen as Auxiliary Reagent. *Microchemical Journal*, **99**, 193-196. https://doi.org/10.1016/j.microc.2011.05.002

[64] https://www.laboreszkozkatalogus.hu/prospektus/Milestone/Milestone-MicroSYNT

H-EN.pdf

[65] Miglietta, M.L. (2023) Private Communication via Research Gate Regarding Type of Microwave Oven and Process Conditions Used.

[66] Öhrngren, P., Fardost, A., Russo, F., Schanche, J.S., Fagrell, M. and Larhed, M. (2012) Evaluation of a Nonresonant Microwave Applicator for Continuous-Flow Chemistry Applications. *American Chemical Society*, **16**, 1053-1063. https://doi.org/10.1021/op300003b

[67] Law, V.J. (2008) Process-Induced Oscillator Frequency Pulling and Phase Noise within Plasma Systems. *Vacuum*, **82**, 630-638. https://doi.org/10.1016/j.vacuum.2007.10.001

[68] Amry, A.M.A., Law, V.J. and Boyd, I.W. (2012) Optical Emission Analysis of Molecular Nitrogen by Using a Self-Resonating Dielectric Barrier Plasma Reactor. *Chinese Physics Letters*, **29**, Article 055201. https://doi.org/10.1088/0256-307X/29/5/055201

[69] Zhang, J.H., Zhang, C. and Zhu, H.C. (2020) A Temperature-Control System for Continuous-Flow Microwave Heating Using a Magnetron as Microwave Source. *IEEE Access*, **8**, 44391-44399. https://doi.org/10.1109/ACCESS.2020.2978124

Appendix

Table A1. Names of Au, Ag, Cu, and Si precursor, solvents, and agents listed in this study. Agents listed in order of carbon atoms.

Chemical name	Abbreviated name	Molecular formula	Purpose of use
Metal precursors			
Choloroauric acid		$HAuCl_4{\cdot}4H_2O$	Au precursor
Silver Nitrate		$AgNO_3$	Ag precursor
Copper Acetate		$Cu(CH_3O_2)_2$	Cu precursor
Silicon precursor			
Tetraethylorthosilicate	TEOS	$Si(C_2H_5O)_4$	Si precursor
Solvents			
Water		H_2O	Solvent, polarity index = 9
Ethanol		C_2H_5OH	Solvent, polarity index = 5.2
Agents			
Sodium borhydride		$(NaBH_4)$.	Reducing agent
Trisodium citrate	Na_3Ct, citrate	$Na_3C_6H_5O_7$	Reducing and stabilizing agent
Oxalic acid		$C_2H_2O_4$	Reducing agent
Citric acid		$C_2H_4O_2$	Reducing agent
Dimethyl sulfoxide	DMSO	C_2H_6OS	Redirecting and reducing agent
Dimethylformamide	DMF	C_3H_7NO	Reducing agent
Ascorbic acid	A A	$C_6H_8N_6O$	Reducing agent
Polyvinylpyrrolidone	PVP	$(C_6H_9NO)_n$	Stabilization agent
Dextran		$H(C_6H_{10}O_5)_nOH$	Reducing and stabilizing agent
Curdlan	Bacterial exopolysaccharide	$(C_6H_{10}O_5)_n$	Reducing and stabilizing agent
Glucose	Sugar	$C_6H_{12}O_6$	Reducing and stabilizing agent
3-Mercaptopropyl trimethoxysilane	MPTMS	$C_6H_{16}O_3SSi$	Reducing agent
Carboxymethyl cellulose sodium	CMS, or cellulose gum	$C_8H_{15}NaO_8$	Reducing and stabilizing agent
11-azidoundecane-1-thiol		$C_{11}H_{23}N_3S$	Functionalization agent
Maltrose	Malt sugar	$C_{12}H_{22}O_{11}$	Reducing and stabilizing agent
Sucrose	White sugar	$C_{12}H_{22}O_{11}$.	Reducing and stabilizing agent
Oleylamine	OA or fatty amine	$C_{18}H_{37}N$	Surfactant agent
Cetyl-trimethylammonium bromide	CTAB	$C_{19}H_{42}BrN$	Surfactant agent
Carboxymethyl Chitosan	CMCT	$C_{20}H_{37}N_3O_{14}$	Reducing and stabilizing agent